

UWB tomosynthesis of objects in mediums with metal inclusions

V P Yakubov¹, S E Shipilov², D Ya Sukhanov³, I V Minin⁴ and O V Minin⁵

¹ Doctor of Physico-mathematical Sciences, Professor, The Department of radiophysics, Tomsk State University, Tomsk, Russia

² Candidate of Physico-mathematical Sciences, Associate Professor, The Department of radiophysics, Tomsk State University, Tomsk, Russia

³ Doctor of Physico-mathematical Sciences, Professor, The Department of radiophysics, Tomsk State University, Tomsk, Russia

⁴ Doctor of Physico-mathematical Sciences, Professor, Department of metrology and optical technology, Siberian State University of Geosystems and Technologies, Novosibirsk, Russia

⁵ Doctor of Physico-mathematical Sciences, Professor, Department of metrology and optical technology, Siberian State University of Geosystems and Technologies, Novosibirsk, Russia

E-mail: s.shipilov@gmail.com

Abstract. Radiowave tomography of dielectric objects containing metal inclusions is a rather complex problem, since the scattering of waves by dielectric inhomogeneities occurs against the background of substantially stronger reflections from metal parts, even if they are geometrically small. The arising features of obtaining a tomogram in such conditions, including overcoming of disguising by reinforcing ribbons and the appearance of locational shadows at different depths, are discussed in the paper. Herewith principled importance to achieve high focusing of UWB radiation by tomosynthesis is noted on the basis of direct experimental data.

1. Introduction

The detection and visualization of dielectric objects against the background of the masking metal inclusions is one of the complex challenges in the modern theory and practice of non-destructive monitoring, for example, in security systems. If this task is a relatively simple task in a X-ray defectoscopy, of course, on conditions of lack of shadings and if it is possible to implement transmission translucence, then the situation significantly becomes complicated in a radio wave tomography. Metal inclusions give significantly larger reflections than dielectric ones, and small responses from them are just lost on a large disturbing background. So, for example, x-ray methods are not very effective when probing cargo in massive cars (figure 1). Special services have to be content with using mechanical probes.





Figure 1. The hidden dielectric object in a metal body at the point of inspection.

The radio wave tomography is based on the solution of the inverse problem of probing of various objects by means of radiowaves. Herewith, the backscattering case is considered similarly to how this task is set in radiolocation, i.e. the reflected or disseminated back radiation is used. Unlike radiolocation the radio tomography is carried out at rather small distances – in a zone of diffraction of Fresnel. The main instrument of obtaining detailed images is an aperture synthesis at which the computer focusing of the inverse radiation is used. The spatial resolution, on which herewith one can count, is determined by the minimum wavelength of used radiation, and in the case of UWB radiation - it is determined by the highest frequency in the spectrum of used radio impulses [1-7].

The problems existing here and ways of their decisions are discussed in this paper. The basis is use of the method of the radio wave tomosynthesis consisting in the development of the technology of aperture synthesis in combination with the operated computer focusing on the basis of fast algorithms. The proposed solutions are followed with the results of theoretical pilot studies.

2. UWB tomosynthesis

The main mathematical problem standing for the development of a method of a tomosynthesis consists in obtaining high resolution and at the same time in real time. Let's discuss the proposed solutions.

Computer inverse focusing can be carried out sequentially or in parallel at once on all ranges. Let's explain an essence of the proposed solution in the most prime special case of the homogeneous background environment. If $j(\mathbf{r}_1)$ is a source distribution of the secondary radiation, concentrated in some volume V_1 , then the reflected field created by them in the point \mathbf{r} of the homogeneous environment is defined as

$$E(\mathbf{r}) = \iiint_{V_1} j(\mathbf{r}_1) G_0(\mathbf{r}_1 - \mathbf{r}) d^3 \mathbf{r}_1$$

It is the equation in convolutions. Here $G_0(\mathbf{r})$ is a free space Green function, i.e. the solution of the wave Helmholtz equation for a free space.

Let's present a Green function for the homogeneous background environment in the form of Weyl decomposition on plane waves

$$G_0(\mathbf{r}) = \exp(ik|\mathbf{r}|)/4p|\mathbf{r}| = \frac{i}{(2p)^2} \mathbf{T}\mathbf{T} \frac{\exp\{i(\boldsymbol{\kappa}_\wedge \boldsymbol{\rho} + k_z z)\}}{2k_z} (d^2 \boldsymbol{\kappa}_\wedge).$$

Here $k_z = \sqrt{k^2 - \boldsymbol{\kappa}_\wedge^2}$ represents a longitudinal projection of a wave vector. As a result for a range of space frequencies of the recorded scattering wave field it is possible to write down

$$E(\boldsymbol{\kappa}_\wedge, z) = \mathbf{T}\mathbf{T} \exp\{i\boldsymbol{\kappa}_\wedge \boldsymbol{\rho}\} E(\boldsymbol{\rho}, z) (d^2 \boldsymbol{\rho}_\wedge) = \frac{i}{2k_z} \exp\{ik_z z\} j(\boldsymbol{\kappa}),$$

where

$$j(\boldsymbol{\kappa}) = \mathbf{T}\mathbf{T}\mathbf{T} \int_{V_1} j(\mathbf{r}_1) \exp(i\boldsymbol{\kappa} \mathbf{r}_1) d^3 \mathbf{r}_1 -$$

represents three-dimensional Fourier transform from a spatial distribution of the secondary sources - radiation currents. From here it is possible to write down that

$$j(\boldsymbol{\kappa}) = -2ik_z \exp\{ik_z z\} E(\boldsymbol{\kappa}_\wedge, z).$$

In fact, this is the representation of the solution of 3D tomography. Here it is enough just to carry out a three-dimensional inverse transformation of Fourier. This is the basic idea of the well-known Stolt method [8].

However, two circumstances are necessary to keep in the mind. Firstly, the value $E(\boldsymbol{\kappa}_\wedge, z)$ is calculated in the plane of measurements remote on z distance from the plane in which there is the origin of coordinates to record the distribution of currents source $j(\mathbf{r}_1)$. Secondly, the right-hand part of the ratio is received for the frequency ω and in the field of two-dimensional space frequencies $\boldsymbol{\kappa}_\wedge = (k_x, k_y)$. The left-hand part contains three-dimensional space frequencies $\boldsymbol{\kappa} = (k_x, k_y, k_z)$,

where $k_z = \sqrt{(\omega/c)^2 - \boldsymbol{\kappa}_\wedge^2}$. Apparently, a transition from one representation to another is necessary, and it is desirable on the uniform grid of counting. Simple interpolation allows to make it. The uniform grid of frequencies is necessary for using of an algorithm of fast Fourier transform.

The result of the simulation modeling on using of the described procedure of restitution of sources, i.e. focusings on all depths, is shown in the figure 2. The result of numerical modeling of distribution of a real part of the field of a point source with the coordinates $x = 20^\circ$ cm, $y = 0$ cm and $z = 150$ cm is shown at the upper part of the figure 2a. The distribution of the field on the axis X in the limits of ± 50 cm in the plane $y = 0$ cm in the frequency range from 6 to 12 GHz is calculated. It is the result of the solution of a direct task.

The result of the solution of the inverse task – recovery of the tomogram in the plane $y = 0$ cm is shown in the figure 2b in the form of gradation of gray color. It can be seen that the given inhomogeneity is restored quite unambiguously. In the case of UWB radiation the described method should be applied to each of frequencies, and the received images should be just summarized.

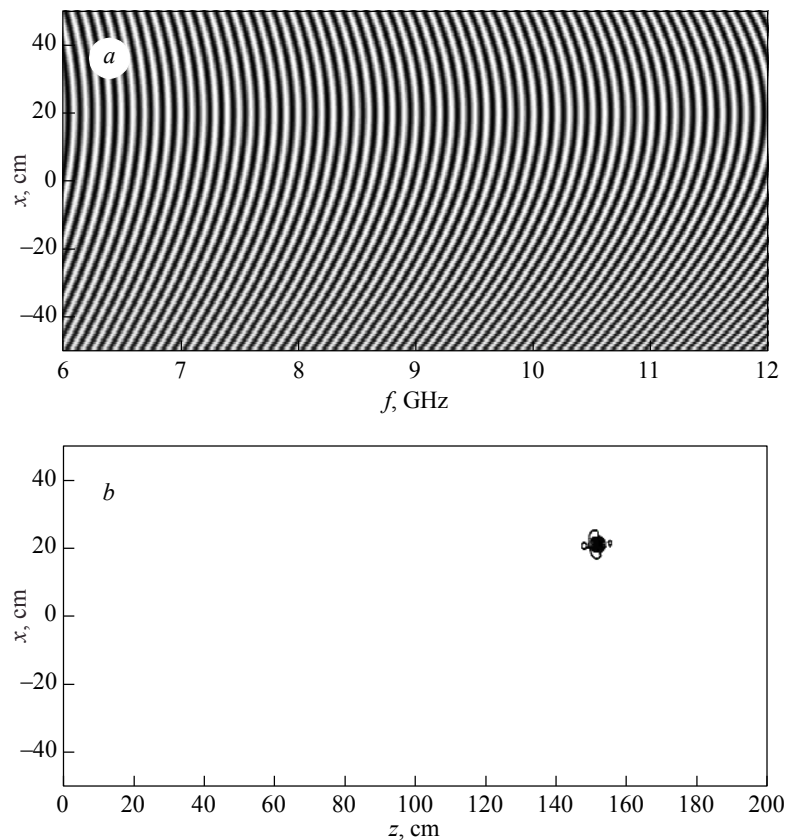


Figure 2. Simulation modeling of a direct (a) and inverse (b) of test tasks.

The model environment from three gas-concrete blocks 10 cm thick each was created for the experimental verification of such approach (figure 3a). A thin test banner of five strips of aluminum foil 2 cm wide each was placed between the 2nd and 3rd layers in the wall from these blocks (figure 3b). The position of the banner is shown by an arrow. The measured index of refraction of aerocrete is established as $n = 1.44$. The result of recovery of the actual radio image of the banner by the explained method is shown in the Fig. 3b in the form of inverse gradation of brightness. Probing was made using UWB-impulses of 200 ps duration. Reasonably accurate reproduction of sizes and mutual arrangement of strips of the banner with a resolution of not worse than 2 cm are observed.

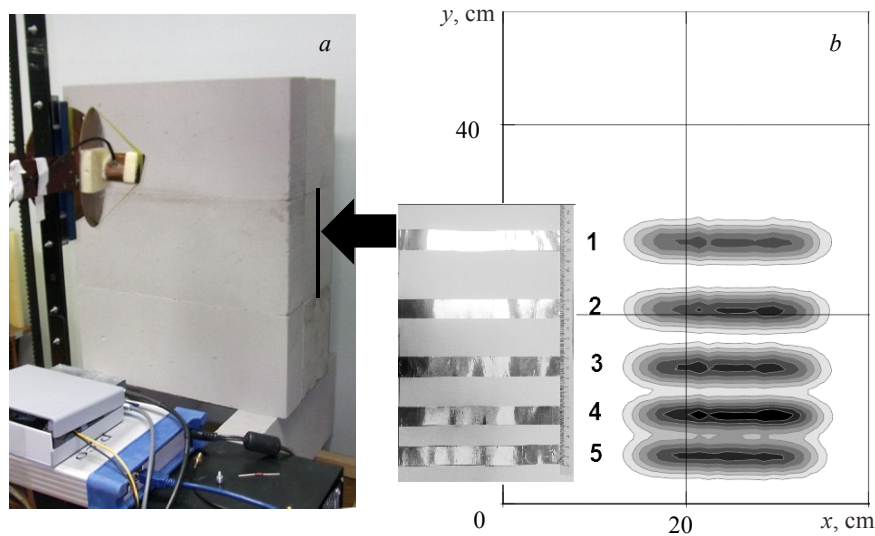


Figure 3. The experimental verification of a tomosynthesis method:
 a – the wall from gas-concrete blocks, b – the test banner and its radio image inside the wall from gas-concrete blocks.

The spatial resolution reached in the method of a radio wave tomosynthesis is quite enough for the solution of the primal problem of this work – of tomography of dielectric objects at the disguising action of metal inclusions.

3. The results of UWB tomosynthesis of objects in mediums with metal inclusions

The method described above was used for tomosynthesis of images of hidden objects in the presence of metallic inclusions. First of all, a wooden packing box reinforced with metal ribbons was subjected to probing (figure 4). A test stepped metallized triangle with the size of each step of 5 cm and with a square hole in the center of 2×2 cm dimension was placed inside the box (figure 5).

Scanning was performed by moving the transceiver antenna module in the OXY plane with the step of 1 cm. The scanning area had dimensions 60×50 cm. The test object was fixed to the bottom of the box at a range of 39 cm, as shown in figure 5. The range is reckoned in the OZ axis direction from the transceiver antenna module.

A 3D-tomogram of the contents of this box with the test object was obtained as a result of UWB-scanning and processing of the received data (figure 6). The reinforcing tape around the perimeter of the cover and a metal handle in the middle of the cover are clearly visible on the section (a), which corresponds to the upper cover of the box at the range of 18.5 cm. Wooden rails on the inside of the front cover of the box can be observed on the section (b), which corresponds to the range of 21.5 cm. The section (c) corresponds to a range of 22.5 cm. The same inhomogeneities are visible in it.



Figure 4. The UWB-scanner and the packing box.



Figure 5. Placing the test object inside the box.

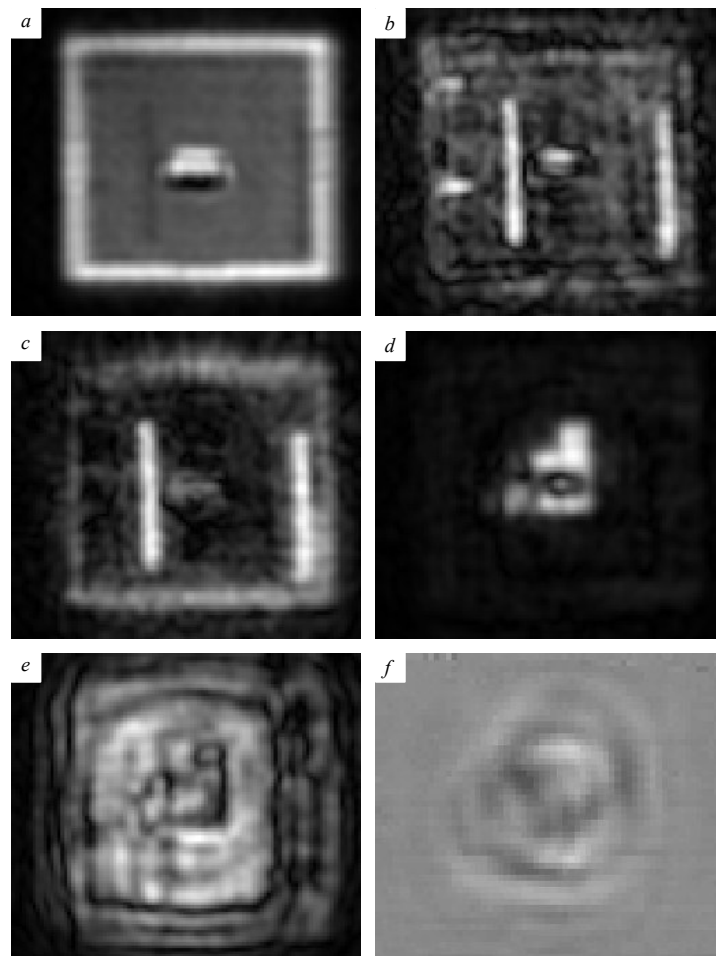


Figure 6. Tomogram of the contents of the reinforced packing box.

The test object, a triangle with a central hole, is visible in the cross-section (*d*) corresponding to the range of 39 cm. Cross-section (*e*) at a range of 42 cm corresponds to the back of the box. The back of the box and a radio shadow from the test object on it are clearly visible on the cross-sections (*d*) and (*e*). The radio shadow appears since the test object is metal-coated and therefore it is not transparent to radio emission.

Thus, according to the results of the experiment, it can be concluded that use of tomosynthesis algorithms allows to be detached from interference caused by the signals reflected from the reinforcing elements. The obtained tomogram allows not only to determine the depth of the hidden test object with an error of not worse than 0.5 cm, but also to visualize its form as well.

Next, let us consider the experimental results of visualization of an objects placed in an open metal container. A metal safe with the dimensions of 64×48×41 cm was chosen for this purpose (see the figure 7). The door of the safe was taken off its hinges.



Figure 7. The test object inside the metal safe.

Based on the scan results, a tomogram of the distribution of inhomogeneities in the tested space was obtained. Radio images of various sections along the range are shown in the figure 8. The figure 8*a* presents the cross-section corresponding to the upper cover of the metal container at the range of 18.5 cm. The front frame of the container is clearly visible on the tomogram. The cross-section corresponding to the range of 19 cm is shown in the figure 8*b*. The indentation used for the container door is visible on the tomogram. The cross-section corresponding to the range of 53 cm is shown in the figure 8*c*. The test object with inside hole is clearly visible on this tomogram. The cross-section at the range of 62 cm is shown in the figure 8*d*. This cross-section corresponds to the back wall of the container.

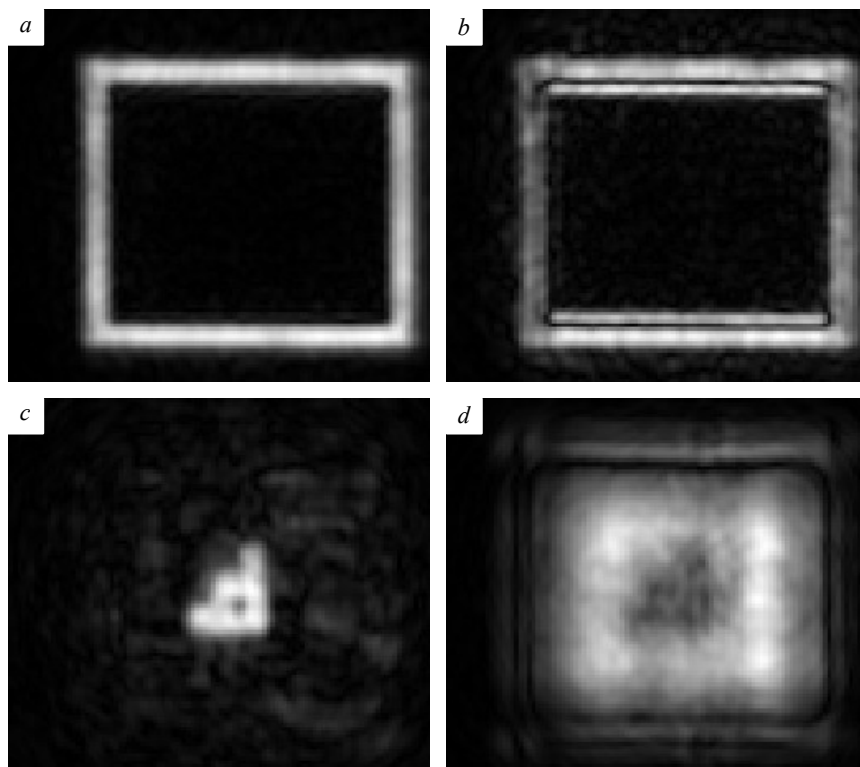


Figure 8. Radio images of sounded area with a metal container at the different ranges.

The main problem at the checkpoints (CP) is the inspection of heavy vehicles for transportation of prohibited items: weapons, explosives, etc. For these purposes there are specialized X-ray equipments, but it is not possible to equip with them all necessary check points because of their high cost. A relatively cheaper radio wave system for the detection and visualization of hidden objects can be used to inspect dump trucks (the figure 1) and other similar techniques. Such system can be a clocked grating of UWB antennas, switching of which is carried out using electromechanical switchboards. The prototype of such grating is shown in the figure 9.



Figure 9. Clocked array of UWB-antennas.

4. Summary

In this work it is shown that the radio tomography of small dielectric and metal objects in the conditions of existence of the masking metal inclusions (reinforcing tapes) and stretched metal walls is

possible with use of UWB pulse radiation when using of the offered method of a radio wave tomosynthesis. The basis for this purpose is made by use realization of the operated existential focusing and fast digital algorithms.

The results are important for creation of perspective customs systems.

Acknowledgments

This research is conducted as part of the Program of Scientific Foundation n.a. D.I. Mendeleev in Tomsk State University - Project No. 8.2.13.2017.

References

- [1] Yakubov V P, Shipilov S E, et al. 2017 *Wave tomography* (Tomsk) p 248
- [2] Satarov R N, Kuzmenko I Yu, Muksunov T R, Klokov A V, Balzovskii E V, Buyanov Y I, Shipilov S E and Yakubov V P 2013 *Russian Physics Journal* **55** 884–9
- [3] Sukhanov D Y and Zav'yalova K V 2015 *The Russian Journal of Applied Physics* **60** 1529–34
- [4] Yakubov V P, Shipilov S E, Sukhanov D Ya and Razinkevich A K 2012 *Russian Journal of Nondestructive Testing* **48** 191–6
- [5] Yakubov V P, Mirontchev A S, Andretsov A G and Ponomaryova I O 2011 *Russian Physics Journal* **53** 895–9
- [6] Yakubov V P, Shipilov S E and Satarov R N 2011 *Russian Physics Journal* **53** pp 887–94
- [7] Shipilov S E, Satarov R N, Fedyanin I, Balzovsky E and Yakubov V P 2016 *MATEC Web of Conferences* **79** 01079
- [8] Stolt R H 1978 *Geophysics* **43** 23–48